DOI: 10.31276/VJSTE.64(3).53-61

Fabrication and structural characterization of self-crosslinking hydrogel based on Vietnamese sources of chitosan and alginate

Tin Dai Luong[1, 2], An Tran-My Le[1, 2], Nhan Thien Vo[1, 2], Thi Hiep Nguyen[1, 2*]

[1]School of Biomedical Engineering, International University, Ho Chi Minh city
[2]Vietnam National University, Ho Chi Minh city

Received 22 April 2022; accepted 11 July 2022

Abstract:

Hydrogel materials have attracted extensive research over the last few decades, especially in tissue engineering, due its many comparable properties with native tissue. This study proposes a new approach to hydrogel fabrication that combines oxidized alginate (OA) into N,O-carboxymethyl chitosan (NOCC) and an oxidized hyaluronan-based hydrogel system employing low cost, domestically sourced chitosan and alginate. Hydrogel fabrication parameters including component ratio and hydrogel concentration were studied. Fourier transform infrared spectroscopy (FT-IR) analysis was applied to confirm the chemical structure of the modified materials. Fabricated hydrogel samples were assessed by cross-sectional surface morphology, equilibrium swelling degree, and *in vitro* degradation behaviour. The results revealed NOCC and oxidized hyaluronic acid (OHA)-OA component contributions toward hydrogel properties, a threshold of raising total polymer content within the network, and a comparison with previous formulations using unmodified alginate. Using low cost domestic resources is a promising way to reduce fabrication expenses, and further work should be performed to evaluate the potential of this cost-effective hydrogel for the tissue engineering field.

Keywords: **carboxymethyl chitosan, oxidized alginate, oxidized hyaluronan, self-crosslinking hydrogel, Vietnamese materials.**

Classification number: **3.6**

Introduction

Hydrogels are unique materials with several desirable properties and they have been applied to a wide range of applications, especially those in the biomedical field [1]. Besides their practical uses as contact lenses and wound dressings, hydrogels have also received considerable attention as a promising scaffolding material for tissue engineering. This area of research aims to create an alternative source of functional grafts to overcome the current gap between transplantation supply and demand [2]. Specifically, hydrogels are formed by crosslinking hydrophilic polymer chains in water, thus, they not only possess an aqueous environment resembling a native extracellular matrix, but also a porous structure for nutrient and waste diffusion during cell culture. Furthermore, control over the transformation from a polymer solution into a gel structure enables, first, minimally invasive injection into complicated defects, secondly, homogeneous delivery of cell and bioactive factors, and, lastly, its potential use as a specialized ink for developing 3D bio-printing technology [3].

Although synthetic polymers are reproducible and exhibit high mechanical stability, only a few of them satisfy the requirements of biocompatibility and appropriate biodegradation, such as poly(ethylene glycol) and poly(N-isopropylacrylamide) [4]. Moreover, synthetic polymer-based hydrogels usually lack the necessary bioactivity while their crosslinking nature, especially polymerization reactions, might employ cytotoxic reagents. Therefore, natural polymers have been extensively targeted as hydrogel components alone or in combination with synthetic polymers [5]. Different crosslinking methods could be employed for natural polymer-based hydrogels, such as the exposure to external stimuli [6], the conventional use of small bi-functional crosslinking agents [7], or the combination of reactive polymers [8]. In the last stated method, two or more hydrogel components with reactive functional groups are prepared independently and allowed to react upon combination. This self-crosslinking approach helps to control the intensity of external factors or the use of additional cytotoxic cross-linkers. Among different types of reactions, Schiff-base reactions stand out as they take place

*Corresponding author: Email: nthiep@hcmiu.edu.vn

under the physiological conditions with rapid kinetics [9]. This reaction requires one component with nucleophilic amino groups (-NH_2) and another with electrophilic aldehyde groups (-CHO), both of which react with each other to form covalent Schiff-base bonds (C=N).

Chitosan, a linear polysaccharide derived from natural chitin by a deacetylation step, is a common material with amino functional groups for Schiff-base reaction-based hydrogels [10, 11]. Chitosan has demonstrated good biocompatibility and low immunogenicity in previous studies. To overcome its drawback of low solubility at neutral pH, chitosan can be grafted with additional carboxylate anions (-COO^-) or quaternized to obtain permanently protonated amino groups (-NH_3^+). NOCC belongs to the former modification technique and is a common constituent for Schiff-base crosslinking reactions since sufficient amino groups remain compared to other grafting techniques targeting N positions. Following chitosan, a second component with aldehyde groups can be achieved by periodate oxidation. It is necessary that the polymer possesses vicinal hydroxyl groups along their chains for the oxidation to take place [9]. Hyaluronic acid (HA), or hyaluronan, is a linear natural polysaccharide that satisfies such a requirement. It exists in the extracellular matrix of human connective tissues, especially cartilage and synovial fluid [12]. Short HA chains have been hypothesized to mediate many biological functions related to proliferation and differentiation of chondrocytes and pro-inflammatory response during wound healing [13]. Modified chitosan has been crosslinked with OHA, such as succinyl chitosan for chondrocyte encapsulation [14], or NOCC for tissue adhesive and dermal wound healing [15, 16]. Despite good healing results, most of these hydrogel formulations exhibit rapid degradation, especially under *in vivo* conditions due to the enzymatic hydrolysis of HA [15]. Therefore, improving the stability of hydrogel containing HA is indispensable to apply this potential biomaterial for tissue engineering field.

Alginate is another linear polysaccharide derived from brown algae with desirable biocompatibility, biodegradability, and low-immunogenicity [17]. It can also be oxidized to crosslink with modified chitosan and has been further combined with bioactive compounds such as albumin for soft tissue engineering [18] and curcumin for dermal wound healing [19]. As a strategy to improve NOCC-OHA hydrogel formulation mentioned above, unmodified alginate was blended into a hydrogel network and an increase in overall stability and degradation time was observed even though the hydrogel concentration remained constant [20]. The given hypothesis was the creation of a more balanced amount of charged groups for a synergistic polyelectrolyte complexation. There is no follow-up study on the effect of oxidizing alginate, which might promote overall crosslink density inside the network and let OA form stronger covalent bonds with NOCC instead of electrostatic interaction.

Herein, a self-crosslinking hydrogel was fabricated based on NOCC, OHA, and OA (Fig. 1). Besides investigating the potential of incorporating OA into the NOCC-OHA network, domestic sources of chitosan and alginate were also targeted to make use of their abundant resource in Vietnam. Different parameters in the hydrogel fabrication process were evaluated including the component ratios and the concentration of polymer content. Modified structures were analysed by FT-IR and viscosity measurements while fabricated hydrogel samples were characterized by scanning electron microscopy (SEM) observation, equilibrium swelling degree, and *in vitro* degradation tests.

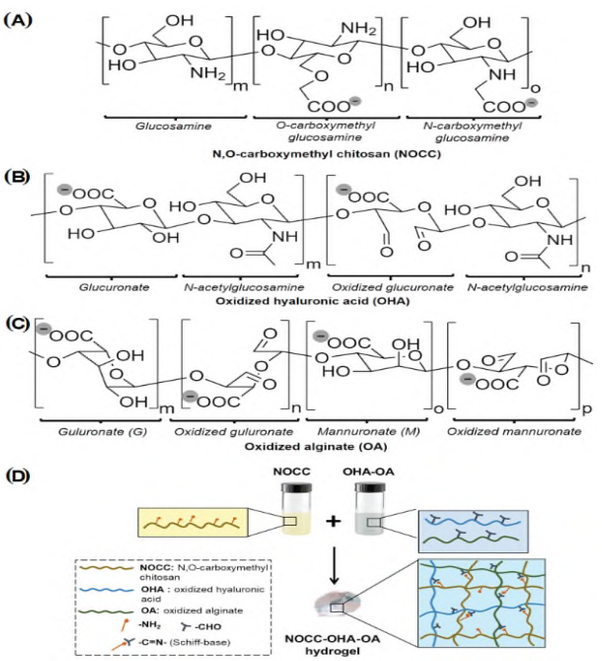

Fig. 1. Chemical structures of (A) NOCC, (B) OHA, (C) OA, and (D) crosslinking mechanism of NOCC-OHA-OA hydrogel.

Materials and methods

Materials

Chitosan derived from shrimp shells with high, medium, or low molecular weight were purchased from Vietnam Food JSC. (Vietnam). HA was purchased from Shandong Bouliga Biotechnology Co., Ltd. (China). Alginate derived from brown seaweed *Sargassum mcclurei* was supplied by Nha Trang Institute of Technology Research and Application (Vietnam). Chloroacetic acid was purchased from HiMedia Laboratories Pvt. Ltd. (India). Sodium metaperiodate

(≥99%) was purchased from Thermo Fisher Scientific Inc. (UK). Dialysis bag (MWCO of 14 kDa) was purchased from Sigma-Aldrich Co., LLC (USA). Isopropyl alcohol, sodium hydroxide, hydrochloric acid, and ethylene glycol were purchased from Xilong Chemical Ltd. (China).

Methods

Synthesis and characterization of hydrogel components

Synthesis of NOCC: chitosan from a Vietnamese source with high, medium, or low molecular weights were modified into NOCC based on a prior study [21]. Briefly, 1 g of chitosan was suspended in 5 ml of isopropyl alcohol. Then, 5 ml of aqueous sodium hydroxide solution was added and the entire mixture was placed at room temperature for an hour. Next, 5 ml of chloroacetic acid in isopropyl alcohol was added 5 times every 5 min. The molar ratio between chloroacetic acid and sodium hydroxide was fixed at 0.42 based on previous study, and different concentrations of chloroacetic acid were investigated for optimal solubility. Specifically, the weights of used sodium hydroxide and chloroacetic acid were investigated between 2.5, 3.125, and 3.75 g. Heat (60^{o}C) was applied at the time of chloroacetic acid addition, and the reaction lasted for a total of 3 h. After the reaction step, the mixture was filtered to obtain the solid part. This part was dissolved in distilled water and neutralized with hydrochloric acid solution. The neutral solution was then dialyzed for 3 d against distilled water. After that, it was frozen overnight and lyophilized for at least 36 h using a Freezone 6 l Benchtop Freeze Dry System (Labconco, USA). The obtained NOCC was kept at 2-8^{o}C.

Synthesis of OHA and OA: OHA was synthesized from HA based on a previous study with slight modification [14]. At first, a solution of 1% (w/v) HA was prepared at room temperature. Next, an aqueous solution of sodium metaperiodate ($NaIO_4$) with 40% molar equivalence to HA dimers was prepared in dark condition and added dropwise into the HA solution. The mixture was stirred for 2 h at room temperature with a fully covered container to avoid light exposure. After that, ethylene glycol with 4-fold molar equivalence to $NaIO_4$ was added to quench residual oxidizing reagents. The mixture was stirred for one more hour under the same conditions. The sample was then dialyzed for 3 days against distilled water. The obtained solution was frozen overnight and lyophilized for at least 36 h to achieve the OHA product, which was stored at 2-8^{o}C.

Alginate derived from Vietnamese brown seaweed was used to synthesize OA by a similar oxidation process to OHA. Briefly, a solution of 1% (w/v) alginate was prepared. Then, an aqueous solution of $NaIO_4$ with 20% molar equivalence to alginate monomers was prepared without light exposure and allowed to react with alginate. The conditions for reaction, dialysis, and freeze-drying steps were similar to the OHA modification protocol. Obtained OA was also stored at 2-8^{o}C.

FT-IR analysis: the chemical structures of the modified components were determined using FT-IR spectroscopy by a Vertex 70v spectrometer (Bruker, USA). The measurement was carried out at room temperature on freeze-dried components in the wavenumber range of 4000-600 cm^{-1} against a KBr membrane background.

Viscosity evaluation: the viscosity of NOCC or OHA-OA precursor solutions at different concentrations were evaluated. NOCC solutions were made by dissolving freeze-dried NOCC in distilled water at 3, 4, or 5% (w/v). OHA-OA solutions were made with the same range of concentrations as the NOCC solutions by dissolving lyophilized OHA and OA with a weight ratio of 1:1. The viscosity was determined at room temperature using a DVE-RV viscometer (Brookfield, USA) equipped with a small sample adaptor (SC4-28).

Fabrication and characterization of NOCC-OHA-OA hydrogel

Fabrication of hydrogel samples: each pair of NOCC and OHA-OA solutions at a specified concentration (3, 4, or 5% w/v) were gently combined at a specified volume ratio to enable crosslinking. Five volume ratios of 3:1, 2:1, 1:1, 1:2, and 1:3 were investigated for the hydrogel at 3% concentration from which a narrower range of volume ratios were chosen for the other two concentrations of 4 and 5%. Formation of hydrogel was confirmed by macroscopic observation.

FT-IR analysis: the prepared hydrogel samples were frozen and lyophilized, then investigated with FT-IR under the same conditions as modified components above.

Cross-sectional surface morphology analysis: the cross-sectional surface morphology of hydrogel samples was observed using SEM. Briefly, each freeze-dried sample was sliced to reveal the inner cross-sectional surface. This surface was then coated with a thin layer of gold using a Smart Coater (JEOL, Japan) and observed using a JSM-IT100 microscope (JEOL, Japan) at 10 kV. The pore diameters were analysed using ImageJ software (USA) (n=3, 40 measurements per sample). The results were displayed as mean±standard deviation.

Equilibrium swelling degree measurement: the equilibrium swelling degree of the hydrogel samples in a hydrated state were measured gravimetrically. At first, each sample was prepared and placed in a 24-well plate. Its initial weight was denoted as W_0. The hydrogel was then immersed completely in phosphate-buffered saline (PBS) (1 X, pH=7.4) and incubated at 37^{o}C. Each sample was weighed every hour until it reached the equilibrium state. The weight at that point was denoted as W_s. The swelling degree was

calculated using the following equation:

Equilibrium swelling degree (%)=$(W_s–W_0)/W_0×100$.

The experiment was done in triplicate. The results were displayed as mean±standard deviation.

In vitro degradation assessment

The degradation of each hydrogel sample was measured gravimetrically under simulated physiological conditions of PBS (1 X, pH=7.4) and 37°C as in the previous experiment. Briefly, the initial hydrogel weight was denoted as W_0. Then, the weight was measured every 24 h for 9 days, recorded as W_t (weight on day t). The PBS medium was changed every 3 day. The percentage of remaining weight (W_d, %) at each time point was calculated using the following equation:

$W_d(\%)=W_t/W_0x100$.

The test was conducted in triplicate. The results were expressed as the mean±standard deviation.

Statistical analysis

All statistics were performed using OriginPro (USA). Results were reported as mean±standard deviation (SD). One-way ANOVA was used to compare the effect of one variable between multiple groups, while two-way ANOVA and Tukey's post hoc test were applied to compare effects of multiple variables. The level of significance was set at $p<0.05$.

Results and discussion

Synthesis of NOCC

Although direct employment of chitosan has been explored in previous studies like crosslinking with benzaldehyde-grafted zinc phtalocyanines [22] or cuminaldehyde [23], the use of acidic solvents to dissolve raw chitosan is not appropriate for cell encapsulation to target tissue engineering. Carboxymethylation was thus performed to acquire a more soluble chitosan derivative NOCC. This substitution reaction took place between a nucleophilic O atom of hydroxyl or N atom of amino groups on chitosan and electrophilic C atom of chloroacetic acid in a polar protic solvent of water and isopropanol [24]. The conditions for this reaction might vary according to the source of chitosan, as each source differs in many respects especially molecular weight, degree of deacetylation, and crystallinity. Our group has determined that the quantities of chloroacetic acid and sodium hydroxide are key parameters of the reaction, which affects the solubility of obtained NOCC [25]. Altering the chloroacetic acid amount changes the grafting degree of charged carboxymethyl groups onto chitosan chains. Besides, an alkaline environment facilitates this grafting reaction, so the amount of base should be raised whenever the amount of acid reactant is increased to ensure a sufficiently high pH value. For imported high-cost chitosan, the most suitable amounts of both acid and base were found to be about 2.5 g per 1 g of chitosan, which yields NOCC product that is soluble up to 5% concentration (w/v) [25]. Based on that result, an investigation into reactant quantities was conducted using Vietnamese low-cost chitosan with different molecular weights. Solubility of obtained NOCC was evaluated after the filtered product reached the dissolution and neutralization steps.

Regarding the high molecular weight source, a wide range from 1.25 to 5 g of reactants were investigated. Representative images of the NOCC solution formulated with 2.5, 3.75, and 5 g of reactant are shown in Fig. 2. Although the solubility of NOCC improved with the increase in reactant, aggregates of insoluble chitosan were observed in the solution with 5 g reactant. For the medium molecular weight source, more distinct results were obtained for a smaller range of 2.5, 3.125, and 3.75 g of reactant. A transition from 2.5 to 3.125 g showed lower amounts and smaller sizes of insoluble chitosan flakes. These observed aggregates were also reduced compared to previous samples from the high molecular weight source, which might be attributed to the higher reaction efficiencies of smaller polymer chains. A further increase to 3.75 g did not demonstrate significant difference in solubility. With regard to the low molecular weight source, repeated amounts of 2.5 and 3.125 g of reactant were applied. However, the solubility of the obtained NOCC did not considerably exceed that of the medium molecular weight. Therefore, this source of chitosan was chosen to reinforce the hydrogel network compared to lower one, while the quantity of 3.125 g of chloroacetic acid and base was employed instead of 3.75 g for a milder use of chemicals with equivalent result. The small amount of aggregates was filtered before the dialysis step to collect solely NOCC products.

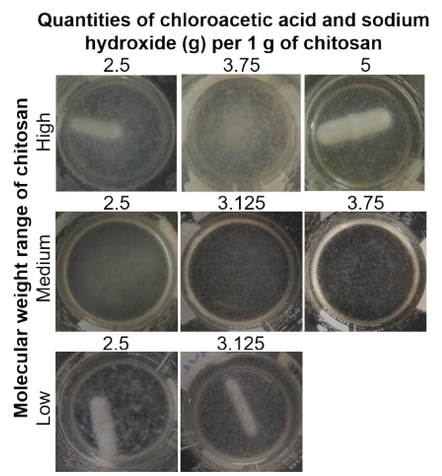

Fig. 2. Top view of NOCC solution obtained from chitosan with high, medium, and low molecular weight using different quantities of chloroacetic acid and sodium hydroxide (g) per 1 g of raw chitosan in the reaction.

FT-IR spectroscopy was used to confirm the modification of chitosan into NOCC. The spectrum of NOCC (Fig. 3) demonstrated emerging broad bands at 1580 and 1403 cm^{-1} of $-COO^-$ antisymmetric and symmetric stretching vibrations, which confirms the appearance of grafted carboxylate groups. These signals overlapped with some original bands of chitosan such as the C=O stretching vibration of amide I (1649 cm^{-1}) and N-H bending vibration of the primary amino group and amide II (1568 cm^{-1}) [26]. Although carboxymethyl groups were partially grafted on reactive amino groups for Schiff-base reactions, a previous investigation [24] showed that this modification took place mostly at the O-position instead of the N-position.

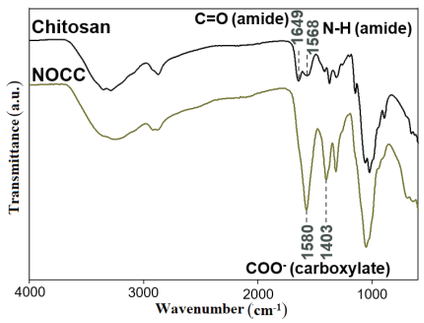

Fig. 3. FT-IR spectra of chitosan and NOCC.

Synthesis of OHA and OA

HA and alginate were oxidized to OHA and OA, respectively, to participate in the crosslinking reaction with NOCC via aldehyde groups. Periodate served as the oxidizing agent that selectively converted vicinal diols along polysaccharide chains into separate di-aldehydes. Unlike the synthesis of NOCC, the molar ratio was fixed between this oxidizing agent and saccharide unit containing vicinal diol, thus, the same amounts of reactants were employed regardless of material source.

As shown in Fig. 4, the spectra of both OHA and OA mostly resembled the original unmodified spectra with the exception of a new shoulder peak around 1730 cm^{-1} representing the C=O stretching vibration of aldehyde. Normally, a C=O stretching vibration yields strong signal owing to the large dipole moment of the bond nature. However, several nearby hydroxyl groups along carbohydrate chains could react with free aldehydes to establish reversible hemiacetals, which lowers the signal intensity. This observation was comparable to FT-IR results from other published studies that showed shoulder peak of aldehyde group between 1721 and 1740 cm^{-1} for oxidized hyaluronan and alginate [15, 27].

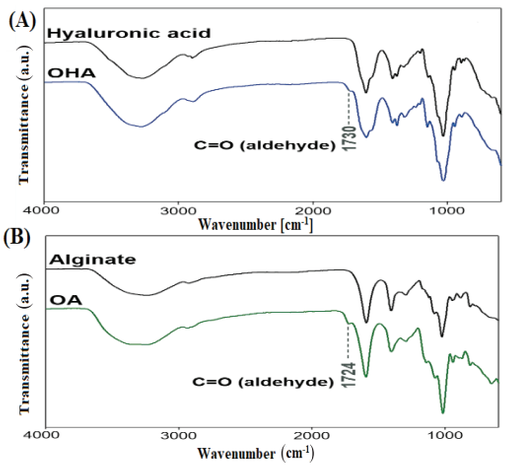

Fig. 4. FT-IR spectra of (A) HA and OHA and **(B)** alginate and OA.

An oxidation degree of 40% for OHA was chosen based on previous studies that compared a close range of degrees around 40% and showed that 40% yielded closer actual values [15] and more desirable properties including biocompatibility [16]. A corresponding degree of 20% was chosen for alginate, as each monomer unit on the alginate structure could be oxidized rather than a dimer unit like HA. Periodate-based oxidation is associated with partial chain cleavage because the obtained aldehyde derivative is more susceptible to alkaline β-elimination and radical depolymerization compared with the original polysaccharide [28]. Therefore, a choice of low oxidation degrees could prevent this chain cleavage problem.

Viscosity evaluation of NOCC and OHA-OA solutions

NOCC and OHA-OA solutions were prepared at different concentrations ranging from 3 to 5% (w/v) for viscosity measurements. OHA and OA were dissolved together at a weight ratio of 1:1 as they both possess aldehyde groups and were expected to react simultaneously with NOCC upon combination. As shown in Fig. 5, an increase in concentration of both solutions led to an increase in viscosity, which was expected. The transition from 3 to 5% led to a 10-fold increment in viscosity for NOCC and 6-fold increment for OHA-OA. In comparison, OHA-OA solutions showed lower viscosity values than NOCC solutions at all concentrations, which was mostly attributed to the difference in intermolecular forces throughout the polymer network of each solution. NOCC possesses both positively charged protonated amino groups ($-NH_3^+$) and negatively charged carboxylate groups ($-COO^-$) at near neutral pH, which form numerous electrostatic interactions between NOCC chains. On the other hand, both OHA and OA only exhibit carboxylate anions possessing weak electrostatic interactions with mobile cations like Na^+.

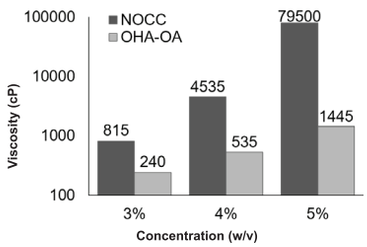

Fig. 5. Viscosity of NOCC and OHA-OA solutions at different concentrations.

Fabrication of hydrogel samples

Following the preparation of NOCC and OHA-OA solutions, different hydrogel samples were fabricated by combining these precursor solutions at a predetermined concentration and volume ratio. The influence of concentration on the hydrogel network were investigated between 3, 4, and 5% (w/v). Regarding the next parameter, as exact moles of amino and aldehyde groups on large polymer molecules are hard to accurately quantify, a common alternative utilizing a component ratio within the network to reflect molar ratio of those functional groups was employed. When the components were combined at an actual molar ratio close to 1:1, the gel network reached its highest crosslink density.

For 3% hydrogel, a wide range of volume ratios were examined between the NOCC and OHA-OA solutions, specifically, 3:1, 2:1, 1:1, 1:2, and 1:3. The hydrogel structure gradually stabilized from a 3:1 ratio to 1:1 ratio, and then became weaker for ratios 1:2 and 1:3. As the two extremes (3:1 and 1:3 ratios) showed unstable hydrogel shapes with long gelation time, the three intermediate ratios of 2:1, 1:1, and 1:2 were used to investigate the 4 and 5% concentrations. At 4% concentration, the increases in viscosities of two precursor solutions started to hinder the handling step of hydrogel combination and mixing. At this concentration, the 1:1 and 2:1 ratios appeared equivalently stable. Regarding the 5% concentration, a 2:1 ratio demonstrated a more stable structure compared to the 1:1 and 1:2 ratios. Considering that the same component ratio should yield equivalent molar ratios regardless of concentration factor, the shifting stability from a 1:1 ratio of 3% and 4% hydrogel to a 2:1 ratio of 5% hydrogel might be attributed to an additional effect from the hydrogel component. The NOCC solution at 5% concentration showed a large viscosity variance with OHA-OA solution and thus its higher proportion might partially contribute to the stability of the network by physical interactions alongside expected covalent crosslinking.

A representative spectra of hydrogel samples at 3% concentration and volume ratios of 1:2, 1:1, and 2:1 are shown in Fig. 6. All hydrogel spectra seemed to inherit most of the peaks from its constituents including NOCC, OHA, and OA. The desirable C=N peak of a Schiff-base bond around 1650 cm^{-1} [29, 30] was not distinctly observed, as it was overlapped by the adjacent stronger and broader $–COO^-$ antisymmetric stretching peak of carboxylate around 1590 cm^{-1}. Nonetheless, the small carbonyl band of aldehyde around 1730 cm^{-1} from the OHA and OA spectra disappeared from the hydrogel spectra, which is evidence that these aldehyde groups participated in the crosslinking reaction. Besides this covalent bond, other physical interactions are also established in the hydrogel network despite not being observed through FT-IR technique including hydrogen bonds and electrostatic interactions between polar or charged groups like hydroxyl, carboxyl, amino, and carbonyl.

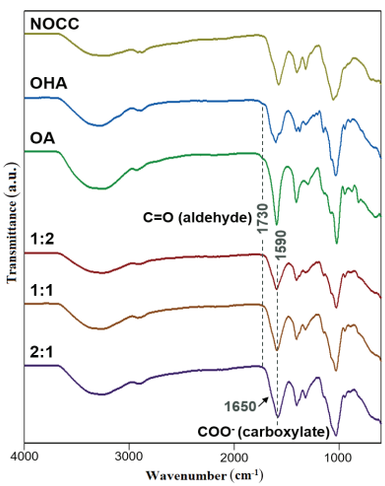

Fig. 6. FT-IR spectrum of NOCC, OHA, OA, and hydrogel samples at 3% concentration and volume ratios of 1:2, 1:1, and 2:1 between NOCC and OHA-OA solutions.

Cross-sectional surface morphology analysis

Morphologies of the cross-sectional surfaces were observed using SEM, and the representative images are presented in Fig. 7. By subjecting hydrogel samples to deep freezing and lyophilization, the inner ice crystals sublimated, leaving a porous network of polymer chains behind. An investigation into surface smoothness, pore shape, and pore size of the cross-sections reflects corresponding homogeneity of the crosslinking process and stiffness of the hydrogel system.

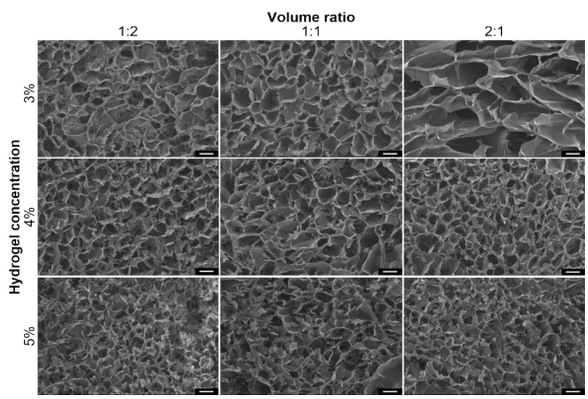

Fig. 7. SEM images of cross-sectional surface of hydrogel samples at magnification of 100X (scale bar of 100 µm).

Overall, the samples exhibited distinct pores to be examined. Among the three tested concentrations, the 3% sample showed more stable pore structures. Appearance of disrupted small holes on the pore surface, along with more disarranged pore shapes, could be observed on the 4 and 5% samples. This heterogeneity might be attributed to a more difficult mixing step at higher viscosity. Besides the influence of concentration, volume ratio was another factor that affected pore size and surface stability according to SEM results. Samples at a 1:2 ratio demonstrated a higher chance of interruption throughout the surface, and a larger diameter was seen for the 2:1 ratio at 3% concentration. In contrast, the other two ratios exhibited higher stability, especially for samples at 3 and 4% concentrations.

A more detailed analysis of pore size was made by measuring the pore diameter of the obtained images and then expressing the results in terms of size distribution and mean value comparison, as shown in Figs. 8 and 9. Considering the distribution curve of all samples, most of them showed a homogeneous range of pore sizes, except for 3% sample at 2:1 ratio. This sample also exhibited a significant increase in average pore diameter compared to other ratios of the same concentration (168 µm versus 103 and 105 µm). Based on these observations, the sample with 1:1 ratio seemed to be the structure with highest crosslink density for 3% concentration owing to its lower pore size, homogeneous size range, and more intact surface. The sample with 4% concentration and 1:1 ratio demonstrated significantly higher pore diameter compared to the 1:2 and 2:1 ratios. Combined with previously observed surface morphology, a shift of stability towards the 2:1 ratio could be noticed as its surface showed less disruptive areas than the 1:2 ratio. Lastly, samples at 5% concentration showed no difference in mean pore diameter between tested ratios, which might indicate their close stiffness.

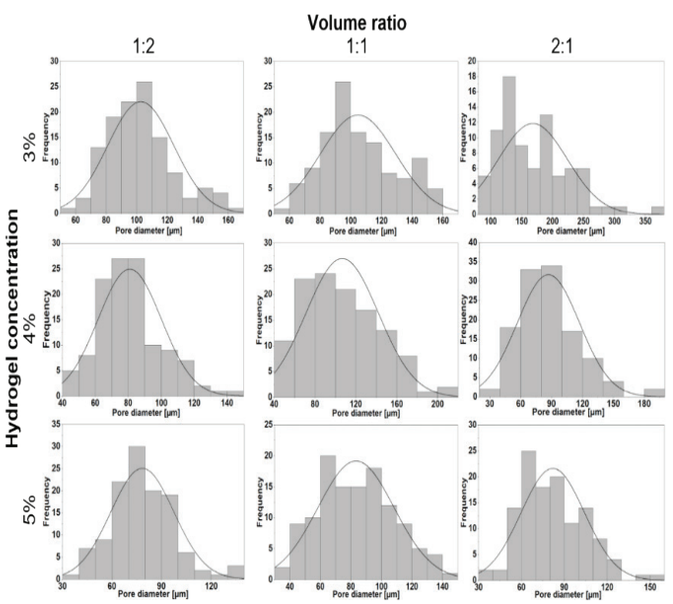

Fig. 8. Pore diameter distribution of cross-sectional surface of hydrogel samples (n=120).

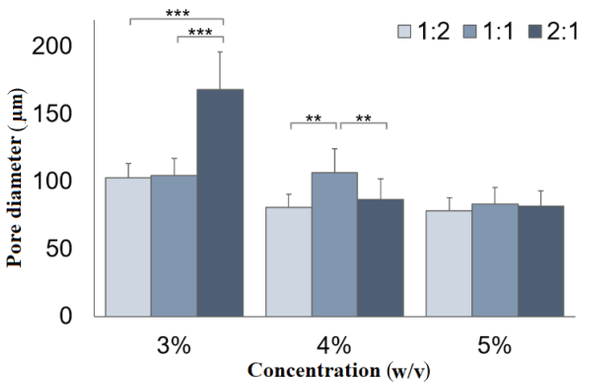

Fig. 9. Pore diameter (µm) of cross-sectional surface of hydrogel samples (values=mean±standard deviation, n=120) (p<0.01, ***p<0.001).**

By comparing samples with similar volume ratios but different concentrations, the influence of concentration on hydrogel morphology was assessed. A significant decrease in pore diameter was noticed when increasing sample concentration from 3 to 5% for all ratios ($p<0.001$). This could be explained by the increasing polymer content in the network leading to more a stable and stiffer structure.

Equilibrium swelling degree measurement

Hydrogel volume change under physiological environment served as an essential factor for practical application of hydrogel. For example, a structure enlarged too much might exceed permissible space at defect site. Swelling behaviour in simulated physiological condition of PBS 1 X at 37°C was monitored for all hydrogel samples. The calculated equilibrium swelling degrees of those samples are presented in Fig. 10. An increase in NOCC component within hydrogel network seemed to correlate with a corresponding increase in hydrogel swelling capacity for 3 and 5% samples. Specifically, 3% hydrogel with 1:2 ratio reached 87% swelling degree, which is significantly lower than 149% of 1:1 ratio. Similarly, the equilibrium swelling degree was 121% for 5% hydrogel with 1:2 ratio, and

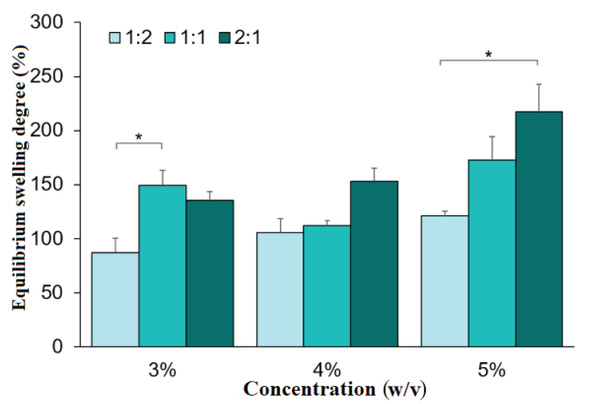

Fig. 10. Equilibrium swelling degree of hydrogel samples at physiological conditions (values=mean±standard deviation, n=3) (*p<0.05).

a significant increase to 217% was observed for 2:1 ratio. The likely explanation for this phenomenon is that the higher NOCC proportion is, the higher amount of charged groups exists inside the hydrogel network. This is associated with a higher inward diffusion from surrounding liquid. This result did not demonstrate the same trend as previous pore diameter graph. Therefore, the swelling capacity of hydrogel based on charge-carrying polysaccharides might depend mostly on inherent characteristic of composition inside hydrogel structure rather than crosslink density and stiffness as in SEM result. Another evidence for the claim above is that altering concentration showed no significant effect on the equilibrium swelling degree of hydrogel regarding all tested volume ratios.

In vitro degradation assessment

Degradation kinetic is a crucial characteristic to consider the balance between degradation rate of scaffold and ECM deposition rate of host cells. Degradation behaviour of hydrogel samples under physiological condition was plotted against the function of incubation time over the course of 9 days as shown in Fig. 11. After reaching equilibrium swelling with the surrounding environment, hydrolysis of Schiff-base bonds and glycosidic bonds took place, which led to eventual degradation of the polymer network. It is noticeable that 3% hydrogel degraded much more rapidly over 6 days compared to the other two concentrations. No significant difference was observed between 4 and 5% hydrogels, as their weights remained approximately 30% compared to the first day. Despite the fact that higher stiffness was observed for 5% hydrogel based on cross-sectional morphology result, an increase in polymer content was not associated with benefits of longer degradation, which might indicate 5% as a threshold for concentration of the proposed hydrogel system. This threshold might be partly attributed to the massive increase in viscosity of precursor solutions, which probably hindered efficient interaction and crosslinking between reactive polymers. On the ninth day, although there was no significant effect of component ratios on degradation rate of the 5% hydrogel, a significantly higher weight remaining was observed for the same with ratio of 2:1 at 4% hydrogel. This sign of improved stability correlated with the result of cross-sectional surface morphology above, despite that this sample may attain high equilibrium swelling degree within the first few hours.

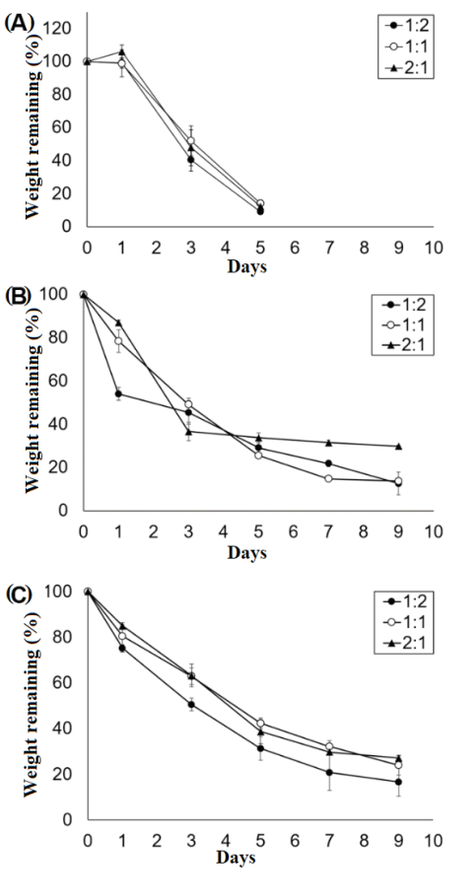

Fig. 11. Degradation kinetic of hydrogel samples at concentration of (A) 3%, (B) 4%, and (C) 5% in physiological conditions within 9 days (values=mean±standard deviation, n=3).

Based on results of morphology, swelling, and degradation behaviour, the ratios of constituents and hydrogel concentration affected the stability of acquired hydrogel network. A concentration of 4% was sufficient to impart higher crosslink density and longer degradation duration without facing many difficulties with handling the highly viscous precursor solutions. A volume ratio of 2:1, which is associated with a higher proportion of NOCC within the network, demonstrated the best stability of obtained hydrogels at 4% concentration. Increasing NOCC content possibly balanced the molar ratios of reactive groups, and simultaneously added more rigid polymeric coils into the structure compared to weaker chains of OHA and OA. Although the incorporation of OA showed faster degradation compared to unmodified alginate in a previous study [20] in which all investigated formulations remained more than 40% of their initial weight on the ninth day, further work should be implemented to fully understand other aspects such as injectability and biocompatibility. One probable explanation for the observed higher degradation kinetic is the cleavage of alginate chains due to the oxidation process, as stated previously.

Conclusions

In summary, NOCC-OHA-OA hydrogels were fabricated based on Schiff-base reaction and characterized in this research, with alteration of firstly component ratios between NOCC and OHA-OA, and secondly the concentrations of hydrogel from 3 to 5%. Different conditions were investigated to synthesize low-cost NOCC from a Vietnamese source, and 3.125 g of both chloroacetic acid reactant and base were chosen. Chemical structures of modified materials were confirmed using FT-IR spectroscopy. Although no direct Schiff-base bond signal was observed on the hydrogel's FT-IR spectra, the disappearance of the aldehyde signal

and macroscopic observation of gelation confirmed the formation of the hydrogel. Although higher concentration contributed higher polymer content for the hydrogel network, 4% was determined as a sufficient concentration to avoid high viscosity concerns. In terms of component ratio, higher NOCC content appeared to impart higher stability into the gel structure and improve long-term degradation, although the corresponding high swelling degree should be considered as well. Based on the obtained results in this study, further works on injectability and biocompatibility should be performed to, first, compare this formulation with one employing unmodified alginate and, second, evaluate this potential polysaccharide-based injectable hydrogel for applications in tissue engineering.

ACKNOWLEDGEMENTS

This research was funded by the Ministry of Science and Technology of Vietnam under grant number DTDL.CN-54/12.

COMPETING INTERESTS

The authors declare that there is no conflict of interest regarding the publication of this article.

REFERENCES

[1] E. Caló, V.V. Khutoryanskiy (2015), "Biomedical applications of hydrogels: A review of patents and commercial products", *European Polymer Journal*, **65**, pp.252-267.

[2] F.J. O'brien (2011), "Biomaterials & scaffolds for tissue engineering", *Materials Today*, **14(3)**, pp.88-95.

[3] I. Armentano, et al. (2010), "Biodegradable polymer matrix nanocomposites for tissue engineering: A review", *Polymer Degradation and Stability*, **95(11)**, pp.2126-2146.

[4] D.M. Radulescu, et al. (2022), "New insights of scaffolds based on hydrogels in tissue engineering", *Polymers*, **14(4)**, DOI: 10.3390/polym14040799.

[5] Y.D. Taghipour, et al. (2020), "The application of hydrogels based on natural polymers for tissue engineering", *Current Medicinal Chemistry*, **27(16)**, pp.2658-2680.

[6] M. Ghorbani, et al. (2017), "Injectable natural polymer compound for tissue engineering of intervertebral disc: *in vitro* study", *Materials Science and Engineering: C*, **80**, pp.502-508.

[7] W.Y. Su, et al. (2010), "Injectable oxidized hyaluronic acid/adipic acid dihydrazide hydrogel for nucleus pulposus regeneration", *Acta Biomaterialia*, **6(8)**, pp.3044-3055.

[8] F. Yu, et al. (2013), "An interpenetrating HA/G/CS biomimic hydrogel via Diels - Alder click chemistry for cartilage tissue engineering", *Carbohydrate Polymers*, **97(1)**, pp.188-195.

[9] J. Xu, et al. (2019), "Hydrogels based on Schiff base linkages for biomedical applications", *Molecules*, **24(16)**, DOI: 10.3390/molecules24163005.

[10] J. Zhang, et al. (2010), "Chitosan modification and pharmaceutical/biomedical applications", *Marine Drugs*, **8(7)**, pp.1962-1987.

[11] R. Antony, et al. (2019), "A review on applications of chitosan-based Schiff bases", *International Journal of Biological Macromolecules*, **129**, pp.615-633.

[12] C. Chung, J.A. Burdick (2009), "Influence of three-dimensional hyaluronic acid microenvironments on mesenchymal stem cell chondrogenesis", *Tissue Engineering Part A*, **15(2)**, pp.243-254.

[13] G. Abatangelo, et al. (2020), "Hyaluronic acid: redefining its role", *Cells*, **9(7)**, DOI: 10.3390/cells9071743.

[14] H. Tan, et al. (2009), "Injectable *in situ* forming biodegradable chitosan-hyaluronic acid based hydrogels for cartilage tissue engineering", *Biomaterials*, **30(13)**, pp.2499-2506.

[15] L. Li, et al. (2014), "Biodegradable and injectable *in situ* cross-linking chitosan-hyaluronic acid based hydrogels for postoperative adhesion prevention", *Biomaterials*, **35(12)**, pp.3903-3917.

[16] N.T.P. Nguyen, et al. (2019), "The effect of oxidation degree and volume ratio of components on properties and applications of *in situ* cross-linking hydrogels based on chitosan and hyaluronic acid", *Materials Science and Engineering: C*, **103**, DOI: 10.1016/j.msec.2019.04.049.

[17] K.Y. Lee, D.J. Mooney (2012), "Alginate: properties and biomedical applications", *Progress in Polymer Science*, **37(1)**, pp.106-126.

[18] L. Xing, et al. (2019), "Covalently polysaccharide-based alginate/chitosan hydrogel embedded alginate microspheres for BSA encapsulation and soft tissue engineering", *International Journal of Biological Macromolecules*, **127**, pp.340-348.

[19] X. Li, et al. (2012), "*In situ* injectable nano-composite hydrogel composed of curcumin, N, O-carboxymethyl chitosan and oxidized alginate for wound healing application", *International Journal of Pharmaceutics*, **437(1-2)**, pp.110-119.

[20] A.N.M. Le, et al. (2020), "Modulating biodegradation and biocompatibility of *in situ* crosslinked hydrogel by the integration of alginate into N, O-carboxylmethyl chitosan-aldehyde hyaluronic acid network", *Polymer Degradation and Stability*, **180**, DOI: 10.1016/j.polymdegradstab.2020.109270.

[21] X.G. Chen, H.J. Park (2003), "Chemical characteristics of O-carboxymethyl chitosans related to the preparation conditions", *Carbohydrate Polymers*, **53(4)**, pp.355-359.

[22] A.R. Karimi, et al. (2016), "A nanoporous photosensitizing hydrogel based on chitosan cross-linked by zinc phthalocyanine: An injectable and pH-stimuli responsive system for effective cancer therapy", *RSC Advances*, **6(94)**, pp.91445-91452.

[23] S. Sharma, et al. (2020), "Dynamic imine bond based chitosan smart hydrogel with magnified mechanical strength for controlled drug delivery", *International Journal of Biological Macromolecules*, **160**, pp.489-495.

[24] V. Mourya, et al. (2010), "Carboxymethyl chitosan and its applications", *Advanced Materials Letters*, **1(1)**, pp.11-33.

[25] N.T.P. Nguyen, et al. (2017), "Synthesis of cross-linking chitosan-hyaluronic acid based hydrogels for tissue engineering applications", *International Conference on the Development of Biomedical Engineering in Vietnam*, **63**, pp.671-675.

[26] E.M. Dahmane, et al. (2014), "Extraction and characterization of chitin and chitosan from Parapenaeus longirostris from Moroccan local sources", *International Journal of Polymer Analysis and Characterization*, **19(4)**, pp.342-351.

[27] L. Pescosolido, et al. (2010), "Injectable and *in situ* gelling hydrogels for modified protein release", *European Biophysics Journal*, **39(6)**, pp.903-909.

[28] K.A. Kristiansen, et al. (2010), "Periodate oxidation of polysaccharides for modification of chemical and physical properties", *Carbohydrate Research*, **345(10)**, pp. 1264-1271.

[29] S. Celik, et al. (2021), "Synthesis, FT-IR and NMR characterization, antibacterial and antioxidant activities, and DNA docking analysis of a new vanillin-derived imine compound", *Journal of Molecular Structure*, **1236**, DOI: 10.1016/j.molstruc.2021.130288.

[30] G. Das, et al. (2014), "Mechanosynthesis of imine, β-ketoenamine, and hydrogen-bonded imine-linked covalent organic frameworks using liquid-assisted grinding", *Chemical Communications*, **50(84)**, pp.12615-12618.